

Discovery of novel FMS kinase inhibitors as anti-inflammatory agents

Carl R. Illig, Jinsheng Chen, Mark J. Wall, Kenneth J. Wilson, Shelley K. Ballentine, M. Jonathan Rudolph, Renee L. DesJarlais, Yanmin Chen, Carsten Schubert, Ioanna Petrounia, Carl S. Cryslar, Christopher J. Molloy, Margery A. Chaikin, Carl L. Manthey, Mark R. Player, Bruce E. Tomczuk and Sanath K. Meegalla*

Johnson & Johnson Pharmaceutical Research & Development, Welsh & McKean Roads, Spring House, PA 19477, USA

Received 14 December 2007; revised 14 January 2008; accepted 15 January 2008

Available online 19 January 2008

Abstract—The optimization of the arylamide lead **2** resulted in identification of a highly potent series of 2,4-disubstituted arylamides. Compound **8** (FMS kinase IC_{50} = 0.0008 μ M) served as a proof-of-concept candidate in a collagen-induced model of arthritis in mice.

© 2008 Elsevier Ltd. All rights reserved.

The colony stimulating factor-1 receptor (CSF-1R, also known as M-CSFR, or FMS) is the exclusive receptor for its ligand, colony stimulating factor-1 (CSF-1 or macrophage colony stimulating factor, M-CSF). The binding of CSF-1 to the extracellular domain of FMS induces the dimerization and trans-autophosphorylation of several cytoplasmic tyrosine residues. These phosphorylated sites function as binding sites for Src homology-2 (SH2) domain-containing signaling proteins which promote gene expression and proliferation. High expression of FMS is limited principally to monocyte/macrophages, oocytes, trophoblasts, mammary epithelium (during lactation), and to cells of the macrophage lineage, while CSF is the predominant growth factor for macrophage lineage cells including osteoclasts.^{1,2} Recent studies have demonstrated a direct correlation between tumor-associated macrophage numbers and tumor progression³ and between synovial macrophage numbers and disease severity in rheumatoid arthritis.⁴ Further, osteoclasts mediate bone erosions leading to pain and fracture in metastatic bone disease and deformity in rheumatoid arthritis.

Hence the inhibition of FMS appears to be of therapeutic value in treating diseases such as rheumatoid arthritis and metastatic cancer to the bone where osteoclasts and macrophages are pathogenic. This hypothesis is also well-supported by the biological studies conducted with CSF-1 deficient mice.^{5–7}

A recent publication⁸ describes the identification of arylamides (**1** and **2**) as FMS inhibitors. Herein we describe the results of further investigation of the SAR of this chemotype and the identification of a potent FMS inhibitor suitable for in vivo studies (See Fig. 1).

In addition to the lead-like properties of the 5-hydroxymethyl compound **2**, it also stabilized an engineered form of the FMS kinase domain⁹ and thereby provided X-ray crystallographic information to guide optimization efforts. It was immediately apparent from the

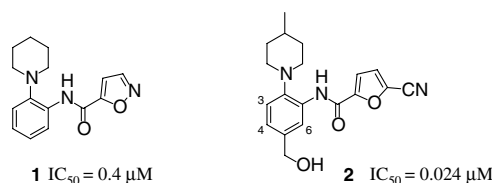
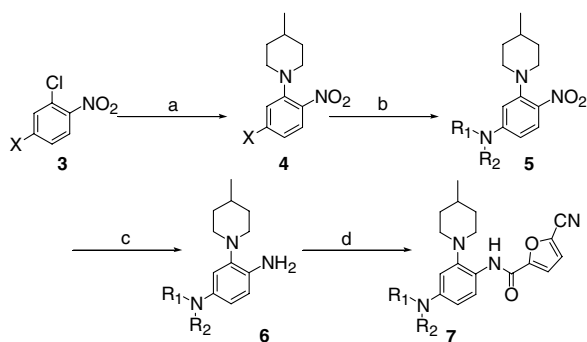


Figure 1. FMS high-throughput screening hit **1** and the lead compound **2**.

Keywords: FMS; CSF-1R; M-CSF; Colony stimulating factor-1; Macrophages; Anti-inflammatory activity.

* Corresponding author. Tel.: +1 610 458 8959; fax +1 610 458 8249; e-mail: smeegall@prdu.snj.com



Scheme 1. Synthesis of 2,4-disubstituted arylamides. Reagents and conditions: (a) 4-methylpiperidine/ rt; (b) R_1R_2NH , THF, reflux 2 h; (c) H_2 , Pd/C, EtOH, rt, 1 h; (d) 5-cyanofuran-2-carbonyl chloride, DCM, Et_3N , rt, 3 h.

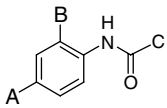
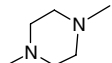
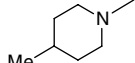
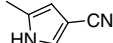
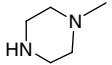
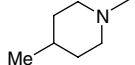
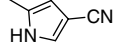
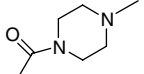
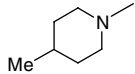
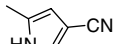
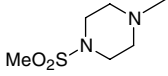
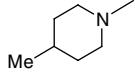
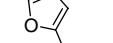
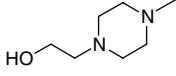
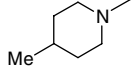
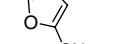
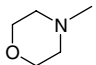
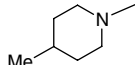
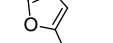
co-crystal structure of FMS and **2** that there was insufficient space at the 6-position of the benzene ring to allow substitution without significant disruption of key binding interactions. Initial efforts geared toward exploring the C-5 position did not lead to further improvement in potency of the lead compound (data not shown). The co-crystal structure of the kinase domain of FMS and **2**⁸ revealed the C-4 position to be a promising site for further elaboration, and optimization efforts began at this site.

The synthesis of compound **7** in Scheme 1 illustrates the general chemistry involved in the synthesis of the 2,4-

disubstituted arylamide chemotype. The initial focus was the introduction of amine substituents at the 2- and 4-positions as the ease of sequential S_NAr reactions on dihalonitrobenzenes permitted rapid analoging for SAR development. Two consecutive S_NAr reactions of 2,4-dichloronitrobenzene **3** ($X = Cl$) with 4-methylpiperidine and a primary or secondary amine in refluxing THF, respectively, installed the desired C-2 and C-4 substituents in high yields. The reduction of the nitro group to the aniline followed by standard amide bond formation with 5-cyanofuran-2-carbonyl chloride afforded the desired final product **7**. Compound **16** was prepared using thiomorpholine as the second nucleophile followed by oxidation prior to acid chloride coupling. Compounds **15** and **20** were prepared employing methylamine as the second nucleophile followed by acylation and sulfonylation prior to the amide bond formation. Compound **19** was made in the same fashion using NH_3 in place of methylamine. Compound **21** was made substituting amine R_1R_2NH with sodium ethoxide. Compound **22** was synthesized by the Sonogashira coupling of propargyl alcohol with intermediate **4** where $X = Br$, followed by Pd-catalyzed hydrogenation, mesylation and substitution of the mesylate with methylethylamine followed by acylation of the resulting aniline.

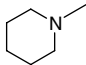
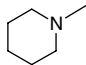
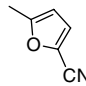
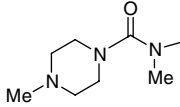
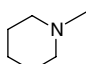
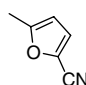
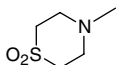
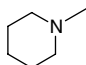
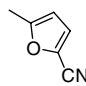
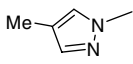
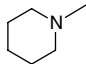
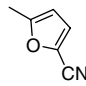
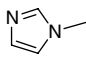
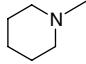
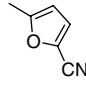
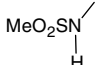
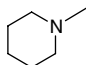
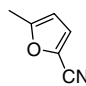
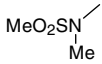
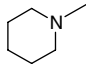
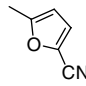
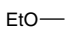
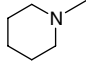
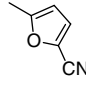
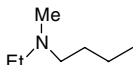
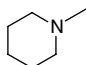
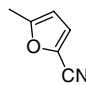
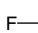
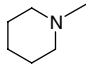
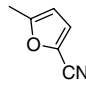
First, the SAR at the C-4 position (Table 1, A) was explored with a variety of N-substitutions, including both saturated and unsaturated N-containing heterocycles. As we have previously reported that both 5-cyanofuran

Table 1. FMS enzyme inhibitory activity¹⁰ for **8–23**

Compound				FMS IC ₅₀ ^a (μM)
	A	B	C	
8				0.0008
9				0.0010
10				0.0007
11				0.0009
12				0.0006
13				0.0110

(continued on next page)

Table 1 (continued)

Compound	A	B	C	FMS IC ₅₀ ^a (μM)
14				0.0170
15				0.0830
16				0.0007
17				0.0640
18				0.0030
19				0.0710
20				0.0250
21				0.0210
22				0.0520
23				0.0630

^aFor assay information see Ref. 10.

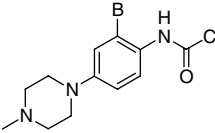
and 4-cyanopyrrole analogues⁸ at the C-1 position exhibited essentially equal potency, a fair activity comparison can be made between cyanofuran and cyanopyrrole analogues.

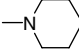
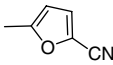
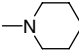
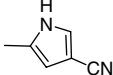
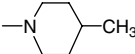
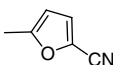
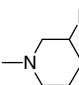
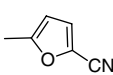
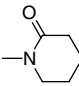
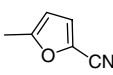
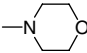
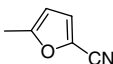
The biological activities of the analogues revealed that the piperazine is a preferred substituent at the C-4 position (8–12). The addition of a methyl group to the 4-piperazine (9 vs. 8) had no effect. Introduction of electron-withdrawing substituents to attenuate the basicity of the piperazine nitrogen also did not have a significant effect on the activity as observed in compounds (10–12). Replacement of basic piperazine at C-4 was detrimental, as seen in morpholine 13, piperidine 14, and pyrazole 17. The replacement of piperazine with imidazole 18 retained activity, though 3-fold less potent than the piperazine analogue 8. The insertion of an amide linker in between the central core and piperazine 15 also exerted a negative effect in the FMS inhibitory activity. The introduction of halides, alkyl and alkoxy substituents and sulfonamides (22, 21, 23, 19 and 20, respectively) resulted in a loss of potency. These results indicate not

only the need for a basic group at the 4-position but a steric requirement that these smaller groups do not fulfill.

The chemistry shown in Scheme 1 was utilized to perform a limited exploration of six-membered N-containing heterocycles at the C-2 position (Table 2, B). The compounds were evaluated in an in vitro FMS assay as well as in a cell-based FMS activity assay (bone-marrow derived macrophage (BMDM) proliferation assay).¹⁰ The data in the Table suggest that small lipophilic groups are tolerated on the piperidine (24–27). The replacement of piperidine with morpholine 29 and piperidinone 28 showed a significant decrease in activity. As reported previously⁸ both 5-cyanofuran and 4-cyanopyrrole analogues at the C-1 position (24 vs 25) exhibited essentially equal potency.

The SAR development in the central ring was carried out by the replacement of the benzenoid ring with various azaheteroaromatic rings. The synthetic routes employed in the preparation of these analogues are

Table 2. FMS inhibitory activity for **24–29**


Compound	B	C	FMS IC ₅₀ ^a (μM)	BMDM IC ₅₀ ^b (μM)
24			0.0008	0.005
25			0.0017	0.002
26			0.0010	0.002
27			0.0063	ND
28			>0.060	>10
29			0.080	2.8

^a For assay information see Ref. 10.^b BMDM- bone marrow derived macrophage proliferation assay. For assay information, see Ref. 8.

shown in [Scheme 2](#). The common synthetic features include two nucleophilic substitutions employing 4-methylpiperidine and 4-methylpiperazine as the nucleophiles with various dichloronitroazaheterocycles (**30**, **36**, **41**, and **46**) and conversion of the nitro functions to amines followed by acylation with 5-cyanofuran-2-carbonyl chloride. The synthesis of the pyrazine analogue **35** was carried out by mono-substitution of 2,6-dichloropyrazine with 4-methylpiperidine followed by nitration of the resulting product to obtain the intermediate **32**. The yield of the formation of this compound was poor

(8%) due to the rapid formation of bisnitro compound. Although the preparation of two pyridyl analogues (**40** and **51**) and the pyrimidine analogue **45** was more straightforward, the synthesis of compound **51** required the preparation of 3,5-dichloro-2-nitropyridine **47**. This compound was prepared in 60% yield by the oxidation of the corresponding amine **46** with Caro's acid, K₂S₂O₈, in concd H₂SO₄. Finally the displacement of the 3-chloro substituent of **47** with 4-methylpiperidine was complicated by the competitive displacement of the 2-nitro group.

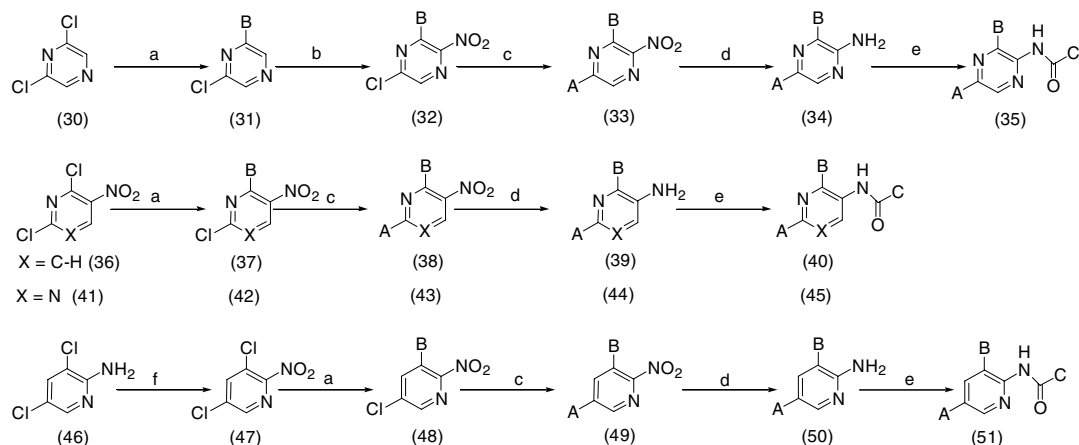
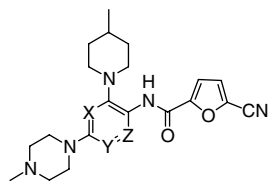
**Scheme 2.** Synthesis of heterocyclic core analogues. Reagents and conditions: (a) 4-Methylpiperidine/THF (b) NO₂BF₄, CH₃CN; (c) *N*-methylpiperazine, THF; (d) Pd/C, EtOH, H₂ (10 psi); (e) 5-cyanofuran-2-carbonyl chloride, Et₃N, DCM; (f) H₂SO₄, K₂S₂O₈, 0 °C → RT, 2 h.

Table 3. FMS inhibitory activity¹⁰ for heterocyclic core analogues


Compound		% Inhibition at 2 μ M	FMS IC ₅₀ (μ M) ^a
26	X = Y = Z = C–H,	100	0.001
35	X = Z = N, Y = C–H,	8	—
40	X = N, Y = Z = C–H,	97	0.01
45	X = Y = N, Z = C–H,	2	—
51	X = Y = C–H, Z = N	69	0.72

^a For assay information see Ref. 10.

The FMS inhibition data¹⁰ for these aza analogues are shown in Table 3. All the heterocyclic core analogues were less active than the corresponding benzenoid counterpart **26**. The presence of a single N in the ring was better tolerated than two and the preferred position of the N appeared to be the 3-position between the two exocyclic nitrogens. However, the most active compound **40** was 10-fold less active than the corresponding benzenoid compound while its regioisomer **51** exhibited 700-fold less potency. The pyrazine and pyrimidine analogues **35** and **45** showed negligible inhibition of FMS at 2 μ M.

Binding models for the interaction of FMS kinase with 4-substituted analogues could readily be built from the published crystal structure of FMS with **2**, PDB ID 2i0y.⁹ Figure 2 shows the model of **26** with FMS. Key interactions include a hydrogen bond between the amide carbonyl and the backbone NH of Cys666 of FMS, an internal hydrogen bond between the amide NH and the O of the furan, and hydrophobic interactions for both the 2- and 4-substituents. The 2-substituent binds in a hydrophobic region made up of the glycine-rich loop on one wall and the side chain of Leu785 on the other. The 4-substituent binds in a relatively hydrophobic region extending out from the ATP-binding site toward solution. The major interaction with the protein is a hydrophobic interaction along the left wall of the site in the lower graphic of Figure 2. The SAR supports this binding mode. We believe that the equivalent potency of the furan and pyrrole groups can be explained by a trade-off of interactions. The furan can accept an internal hydrogen bond from the amide NH, stabilizing the necessary planar conformation, while the pyrrole instead can make an additional hydrogen bond between the pyrrole NH and the backbone carbonyl of FMS residue Glu664. The 2-position has a tight steric fit with only a small amount of room at the 4' site, explaining the loss in activity for substitution at the 2'- or 3'-positions. Hydrophilic substitution at the 4'-position is also not tolerated. At the 4-position, hydrophilic groups placed close to the central ring such as the amide **15**, pyrazole **17**, imidazole **18** or sulfone (**19** and **20**) all dramatically decrease activity. However, polarity is well-tolerated at the 4'-position of the C-4 substituent. This

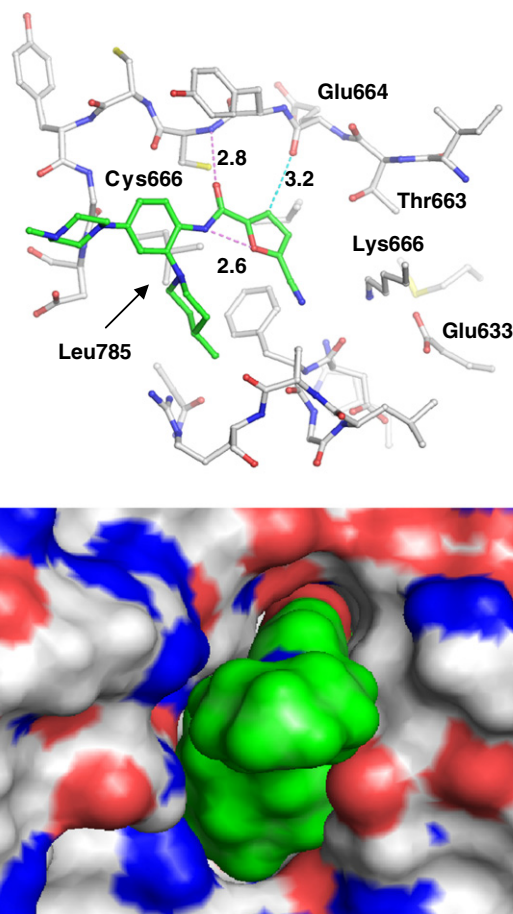


Figure 2. Model of compound **26** (green carbons) bound to the FMS kinase (white carbons). The top graphic shows a cutaway view of the complex, heavy atoms only, with the hydrogen bonds displayed as a magenta dotted line and a potential hydrogen bond displayed as a cyan dotted line. Distances are in Å. The bottom view shows an end-on view of the complex with all atomic molecular surfaces displayed.¹¹

is quite solvent exposed and does not interfere with the hydrophobic interactions of the ring. Acyclic substituents at C-4 are also less active, presumably because they cannot adequately fill the site.

Having successfully achieved good in vitro potency, the pharmacokinetic profiles of several of the more potent compounds (**24**, **26**, and **8**) were evaluated. The pharmacokinetic parameters for these compounds are shown in Table 4. All compounds showed good oral bioavailability in mice ranging from 32% to 45%. However, cyanopyrrole **8** was clearly superior having a longer *t*_{1/2} of 244 min, lower clearance, and moderate volume of distribution; thus it was chosen for further study.

Table 5 shows the kinase selectivity of **8**. Although this compound was highly potent against FMS, it also inhibited the receptor tyrosine kinases Kit, Axl, TrkA, and Flt-3 and IRK- β at concentrations less than 0.1 μ M. However, all other 89 kinases tested were inhibited only at much higher concentrations.

The therapeutic potential of **8** was then evaluated in a murine collagen-induced model of arthritis (CIA). Oral

Table 4. Pharmacokinetic parameters for **24**, **26** and **8**

Compound	$t_{1/2}$ (IV) (min)	C_{max} (ng/ml)	V_{ss} (ml/kg)	Cl	F (%) (ml/min/kg)
24 ^a	62	386	7970	107	32
26 ^b	98	454	11370	42	39
8 ^b	244	853	5635	16	45

Male CD-1 mice dosed 2 mg/kg iv and 10 mg/kg po.

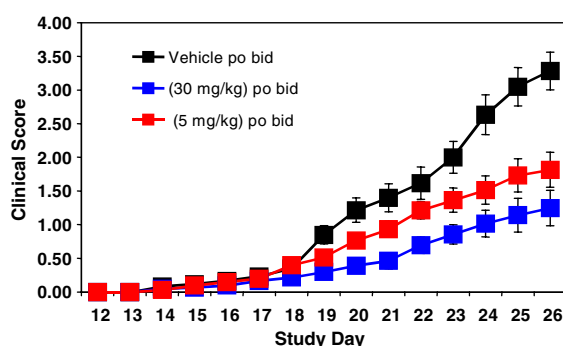
^a 10% DMSO in PEG 400.

^b 20% HP- β -CD.

Table 5. Kinase selectivity of **8**

Kinase	IC ₅₀ ^a (μ M)
FMS	0.00078
Kit	0.0035
Axl	0.0064
TrkA	0.011
Flt3	0.018
IRK β	0.083

^a IC₅₀ values were determined at the respective ATP K_m of each kinase.

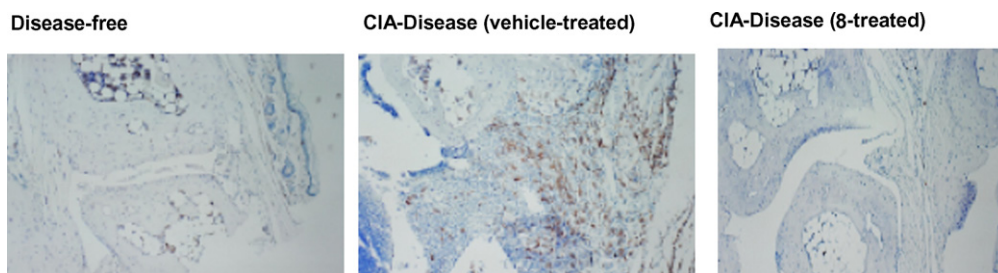
**Figure 3.** Clinical scores for suppression of CIA by **8**.

twice-daily dosing of 30 and 5 mg/kg reduced the overall progression of clinical scores by 65% and 35%, respectively, as shown in Figure 3.

Table 6. Impact of **8** on histopathology of collagen-induced arthritis¹³

	Inflammation mean (SE)	Cartilage damage mean (SE)	Pannus invasion mean (SE)	Bone erosion mean (SE)
Disease-free	0	0	0	0
CIA, Vehicle	3.28 (0.25)	3.16 (0.28)	1.82 (0.25)	1.82 (0.25)
CIA, 5 mg/kg	2.01 (0.24) ^a	1.87 (0.20) ^a	0.75 (0.12) ^a	0.75 (0.12) ^a
CIA, 30 mg/kg	1.54 (0.22) ^a	1.44 (0.21) ^a	0.40(0.10) ^a	0.37(0.11) ^a

^a $p < 0.05$.

**Figure 4.** Selective depletion of macrophages in CIA model by **8**. Paws were fixed, decalcified, and sectioned, and stained for F4/80 positive macrophages. Note the markedly reduced level of F4/80 positive macrophages in the paw of the compound **8**-treated mouse (30 mg/kg).

The therapeutic potential of **8** was then evaluated in a murine collagen-induced model of arthritis (CIA). Oral twice-daily dosing of 30 and 5 mg/kg reduced the overall progression of clinical scores by 65% and 35%, respectively, as shown in Figure 3.

Consistent with the clinical scores, histological examination (Table 6) revealed a reduction of pannus formation and a reduction in the destruction of bone and cartilage. Importantly, pannus growth and bone destruction were reduced by 80%, a level of efficacy comparable to anti-TNF strategies in CIA models.¹² We were also able to show that macrophages were a cellular target of **8** as these cells were depleted from the joints of treated mice (Fig. 4).

In conclusion, optimization of the original lead **2** led to the discovery of a series of potent, orally active, and novel small-molecule FMS kinase inhibitors. One of these, **8**, was employed in an in vivo efficacy study to demonstrate their potential benefit in the treatment of arthritis. These data from the collagen-induced arthritis model in mice showed that the evaluated FMS inhibitor was efficacious in reducing bone erosion, pannus invasion, cartilage damage and inflammation.

In light of the literature precedent for the involvement of macrophages and cells of the macrophage lineage in inflammation, metastatic bone disease, and arthritis, these agents may have good utility for the treatment of these diseases.

References and notes

1. Metcalf, D. The Florey Lecture *Philos. Trans. R. Soc. Lond. B Biol. Sci.* **1991**, 333, 147.
2. Pixley, F. J.; Stanley, E. R. *Trends Cell Biol.* **2004**, 14, 628.
3. Chen, J. J. W.; Lin, Y. C.; Yao, P. L.; Yuan, A.; Chen, H. Y.; Shun, C. T.; Tsai, M. F.; Chen, C. H.; Yang, P. C. *J. Clin. Onco.* **2005**, 23, 953.
4. Haringman, J. J.; Gerlag, D. M.; Zwinderman, A. H.; Smeets, T. J.; Kraan, M. C.; Bateten, D.; McInnes, I. B.; Bresnihan, B.; Tak, P. P. *Ann. Rheum. Dis.* **2005**, 64, 834.
5. Campbell, I. A.; Rich, M. J.; Bischof, R. J.; Hamilton, J. A. *J. Leukocyte Biol.* **2000**, 68, 144.
6. Pollard, J. W.; Stanley, E. R. *Adv. Devel. Biochem.* **1995**, 4, 153.
7. Van Wesenbeeck, L.; Odgren, P. R.; MacKey, C. A.; D'Angelo, M.; Safadi, F. F.; Popoff, S. N.; Van Hul, W.; Marks, S. C., Jr. *Proc. Nat. Acad. Sci.* **2002**, 99, 14303.
8. Patch, R. J.; Brandt, B. M.; Asgari, D.; Baidur, N.; Chadha, N. K.; Georgiadis, T.; Cheung, W. S.; Petrounia, I. P.; Chaikin, M. A.; Player, M. R. *Bioorg. Med. Chem. Lett.* **2007**, 17, 6070.
9. (a) Schubert, C.; Schalk-Hihi, C.; Struble, G. T.; Ma, H. C.; Petrounia, I. P.; Brandt, B.; Deckman, I. C.; Patch, R. J.; Player, M. R.; Spurlino, J. C.; Springer, B. A. *J. Biol. Chem.* **2007**, 282, 4094; (b) Berman, H. M.; Westbrook, J.; Feng, Z.; Gilliland, G.; Bhat, T. N.; Weissig, H.; Shindyalov, I. N.; Bourne, P. E. *Nucleic Acids Res.* **2000**, 28, 235.
10. FMS, FLT-3, KIT, Axl, TrkA and IRK β kinase assays: the full cytoplasmic regions of FMS (538–972) and FLT-3 (571–993) encompassing the tyrosine kinase domains were expressed and purified from a baculovirus system as described Schalk-Hihi, C.; Ma, H. C.; Struble, G. T.; Bayoumy, S.; Williams, R.; Devine, E.; Petrounia, I. P.; Mezzasalma, T.; Zeng, L.; Schubert, C.; Grasberger, B.; Springer, B. A.; Deckman, I. C. *J. Biol. Chem.* **2007**, 282, 4085, KIT, Axl, TrkA, and IRK β were purchased from ProQinase, Upstate, Invitrogen, and BioMol, respectively. FMS 555–568 peptide (SYEGNSYTFIDPTQ) was synthesized and purified by AnaSpec. FMS was assayed using a fluorescence polarization (FP) competition immunoassay that measured FMS phosphorylation of FMS 555–568 peptide at Y561. The reaction mixture (10 μ L) contained 100 mM HEPES, pH 7.5, 1 mM DTT, 0.01% Tween 20 (v/v), 2% DMSO, 308 μ M FMS 555–568 peptide, 1 mM ATP, 5 mM MgCl₂, and 0.7 nM FMS. The reaction was initiated with ATP, incubated 80 min at room temperature, and quenched by the addition of 5.4 mM EDTA. Ten microliters of FP buffer/tracer/phospho-Y antibody mix (Tyrosine kinase assay kit, Green P2837, Invitrogen) was added to the quenched reaction, and FP was measured after 30 min using an Analyst reader (Molecular Devices) at excitation/emission of 485/530 nm. FLT-3, KIT, Axl, TrkA, and IRK β were assayed using the fluorescence polarization competition format as described for FMS except that poly Glu4Tyr (Sigma) was used as a universal substrate. FLT-3 reactions contained 10 nM FLT-3, 113 μ M ATP, and 20 μ g/ml poly Glu4Tyr, incubated for 25 min. KIT reactions contained 1 nM KIT, 50 μ M ATP, and 100 μ g/ml poly Glu4Tyr, incubated for 30 min. Axl reactions contained 0.5 nM Axl, 20 μ M ATP, and 25 μ g/ml poly Glu4Tyr, incubated for 11 min. TrkA reactions contained 5 nM TrkA, 20 μ M ATP, and 20 μ g/ml poly Glu4Tyr, incubated for 27 min. IRK β reactions contained 25 nM IRK β , 50 μ M ATP, and 20 μ g/ml poly Glu4Tyr, incubated for 20 min. IC₅₀s were calculated using GraphPad Prism[®] software and a four-parameter logistics equation. Reported IC₅₀ values are means of at least three experiments. Typical between-run coefficient of variation was less than 20%. Inhibition of 89 other kinases at 1 and 0.1 μ M were conducted by Invitrogen and Millipore kinase profiling services.
11. Figure 2 was prepared with PyMol v0.98. DeLano, W.L. The PyMOL Molecular Graphics System (2002) on World Wide Web <http://www.pymol.org>.
12. Takei, I.; Takagi, M.; Ida, H.; Ogino, T.; Santavirta, S.; Kontinen, Y. T. *J. Rheumatol.* **2000**, 27, 894.
13. The CIA model was performed by Bolder BioPath, Inc., Boulder, CO. Male B10RIII (Jackson Labs) were immunized with type II collagen (Elastin Products), in Freund's complete adjuvant (with supplemental M. tuberculosis, 4 mg/ml, Difco) on Days 0 and 15. On Day 12, animals were randomized by body weight into groups ($n = 15$), and dosing was initiated and continued every day (BID, 12 h intervals) for a total of 14 days. Clinical scores were given for each of the paws (right front, left front, right rear, left rear) as follows: 0 = normal; 1 = 1 hind or fore paw joint affected or minimal diffuse erythema and swelling; 2 = 2 hind or fore paw joints affected or mild diffuse erythema and swelling; 3 = 3 hind or fore paw joints affected or moderate diffuse erythema and swelling; 4 = marked diffuse erythema and swelling, or =4 digit joints affected; 5 = severe diffuse erythema and severe swelling entire paw, unable to flex digits). On day 26, mice were euthanized and paws were fixed in buffered formalin and prepared for histopathology. Inflammation, cartilage damage, pannus invasion, and bone erosion were scored using a 4-point scale.